INTERNATIONAL JOURNAL OF MARITIME TECHNOLOGY
IJMT Vol.15/ Winter 2021 (147-155)

Available online at: www.ijmt.ir

Numerical modeling of armour type and arrangement effects on wave overtopping at rubble mound breakwater

Ali Ghasemi[1*], Rouhollah Amirabadi[2], Ulrich Reza Kamalin[3], Ahmad Rezaee Mazyak [4]

[1] *PhD Candidate, Civil Engineering Department, Faculty of Engineering, University of Qom; ghasemi.ali89@gmail.com*
[2] *Assistant Professor, Civil Engineering Department, Faculty of Engineering, University of Qom; r.amirabadi@qom.ac.ir*
[2] *Assistant Professor, Civil Engineering Department, Faculty of Engineering, University of Qom; ur.Kamalian@gmail.com*
[3] *PhD Candidate, Tarbiat Modares University*; *ahmadrezaee2010@gmail.com*

ARTICLE INFO

Article History:
Received: 04 Sep. 2021
Accepted: 05 Dec. 2021

Keywords:
Rubble mound breakwater
pre-fabricated armour units
overtopping
FLOW-3D software

ABSTRACT

The wave overtopping phenomenon at rubble mound breakwaters is one of the most important issues during the past few years and always plays a unique role in the design process of such structures. Most modeling studies in the overtopping measurment have been based on experimental methods and numerical modeling of wave overtopping from porous breakwater with pre-fabricated armour layer, under irregular waves has been less investigated. In this study, FLOW-3D software was used to calculate overtopping discharge. To assess the accuracy of software results, first, for three of modeled wave heights in the laboratory, numerical modeling was performed and the comparison between numerical and experimental overtopping results showed about 15% error which is acceptable considering the differences between numerical and experimental modeling characteristics, errors and uncertainty in numerical modeling. In the following, numerical modeling for concrete pre-fabricated Xbloc, Antifer, and Tetrapad armour units with different arrangements has been performed. The comparison between results shows that the Antifer armours have the least overtopping and the regular arrangement of Xbloc has the most.

1. Introduction

The Armour layer is the most important section of a rubble mound breakwater because its damage and destruction can destroy other sections of the structure. Armour layer has a crucial influence on the reflection coefficient of the wave, run-up, and the amount of wave overtopping discharge. Wave overtopping phenomenon at rubble mound breakwater is one of the most important issues during the past few years and always plays a unique role in the design process of such structures. Because of uncertainty in the prediction of wave height and the high cost of elevated structure, some percentage of overtopping is unavoidable[1].

Generally, for a specific storm, the total volume of overtopped water is well predictable by Jensen and Van Der Meer (1994), Owen (1980), Hedjes and Reice (1998), formulas which are based on experimental methods; However Goda (2000) has shown that these formulas are not well considered the complexity of wave in shallow waters, and thus, the predicted overtopping discharge could be less than actual amounts. The performed analyses by Besli et al. (1998) have shown that the methods not considering this effect may predict the overtopping discharge less than the actual amount. Numerical studies of Hue et al. (2000) have also approved this fact[2], [3], [4], [5], [6].

With the increasing computational power of computers, more computational models have been developed during recent years, to model wave overtopping at structures. Initial serious efforts in this field were fulfilled by Kobaieshi and Verjantio in 1989. They modeled overtopping of the regular wave at impermeable coastal structures on sloping foreshore[7]. Maroyama and Hirashi (1998) presented a numerical model to calculate the

overtopping discharge of multidirectional waves at a vertical breakwater. The main assumption of this modeling was defining the overtopping discharge by overflow equation[8]. Hue et al. (2000) presented a 2D numerical model to calculate overtopping in shallow water by nonlinear equations, but this study is only valid for regular waves[2]. To 3D modeling and calculate overtopping discharge of irregular waves, the volume of fluid (VOF)-based methods were used. This approach results in a detailed overtopping study process than which is possible in physical model experiments.

One of the well-known VOF-based codes is NASA-VOF2D, which has been revised several times. Develops performed on this code and also SOLA-VOF code has resulted in commercial CFD code called FLOW-3D[9,] [10]. Dental et al. (2012) modeled wave overtopping at rubble mound breakwater subjected to waves from JONSWAP spectrum. They show the results from the software are so close to the experimental study[11].

Ghasemi et al. (2016) by using FLOW-3D software compute the wave overtopping from armour breakwater by considering porous effect.

Milanian et al. (2017) considered the effect of hydraulic and structural parameters on wave run-up on berm breakwater by using FLOW-3D software[13].

Marashian et al. (2018) simulated the wave overtopping over a composite berm breakwater the results of this research shows that wave overtopping over a composite breakwater significantly decreases rather than berm and caisson breakwater[13].

Amirabadi et al. (2018) simulated the investigation of irregular wave interaction with caisson breakwater. They presented the comparison between Owen formula and numerical modeling results of wave overtopping for two different conditions: the breakwater with the porosity of 0.15 and non-porous breakwater[14].

2. Governing Equations

FLOW-3D software is multilateral software that is compatible with complex flow conditions under 2D and 3D modeling. A solution method for equations in this software is based on the finite volume method in the regular mesh.

In the following, the governing equations of fluid flow, turbulence models, and flow modeling in porous media are discussed. The governing equations of fluid flow are indicative of conservation physical laws as mathematical form. One of these laws is continuity equation, which is derived from mass conservation law, by writing mass balance equations for a volume of fluid and assuming fluid incompressibility in three directions x, y, and z as equation (1):

$$\frac{\partial(u)}{\partial(x)}+\frac{\partial(\mathrm{v})}{\partial(y)}+\frac{\partial(w)}{\partial(z)}=0 \tag{1}$$

Where u, v, and w are velocity parameters in x, y, and z directions, respectively.

The other law is momentum conservation or Newton's second law. This law states that momentum change rate equals resultant forces acting on the fluid. Considering incompressible flow and assuming constant viscosity coefficient, the Navier-Stokes equations are as equation (2):

$$\begin{cases}\rho\left(\frac{\partial u}{\partial t}+u\frac{\partial u}{\partial x}+v\frac{\partial u}{\partial y}+w\frac{\partial u}{\partial z}\right)=-\frac{\partial P}{\partial x}+\rho g_x+\mu\left(\frac{\partial^2 u}{\partial x^2}+\frac{\partial^2 u}{\partial y^2}+\frac{\partial^2 u}{\partial z^2}\right)\\ \rho\left(\frac{\partial v}{\partial t}+u\frac{\partial v}{\partial x}+v\frac{\partial v}{\partial y}+w\frac{\partial v}{\partial z}\right)=-\frac{\partial P}{\partial y}+\rho g_y+\mu\left(\frac{\partial^2 v}{\partial x^2}+\frac{\partial^2 v}{\partial y^2}+\frac{\partial^2 v}{\partial z^2}\right)\\ \rho\left(\frac{\partial w}{\partial t}+u\frac{\partial w}{\partial x}+v\frac{\partial w}{\partial y}+w\frac{\partial w}{\partial z}\right)=-\frac{\partial P}{\partial z}+\rho g_z+\mu\left(\frac{\partial^2 w}{\partial x^2}+\frac{\partial^2 w}{\partial y^2}+\frac{\partial^2 w}{\partial z^2}\right)\end{cases} \tag{2}$$

Where g_x, g_y, and g_z are mass accelerations in x, y, and z directions, respectively.

The software allows using several turbulence models including RNG, k-e, and LES. RNG model uses equations similar to the k-e model. As well, LES is more used for modeling large-eddy simulations.

The software uses two methods for porosity modeling, Darcy and Forchheimer. According to Darcy's law, the pressure drop in porous media is related to linear averaged velocity (equation 3). In this equation, k is permeability, μ is dynamic viscosity, and U_D is Darcy velocity of the apparent velocity of flow. Hereby, it is assumed that flow is stable, therefore, the effects of inertia and time dependence have not been considered and thus it is valid for very low Reynolds number (Re < 1).

$$\nabla p=-\frac{\mu}{K}u_D \tag{3}$$

By increasing Reynolds number and pressure drop, the Darcy formula comes out of linear form. Forchheimer added non-linear terms to Darcy's formula and presented equation (4). Forchheimer observed that by velocity increase, inertia effects have been dominant on flow.

$$-\nabla p = (a + b|u_D|)u_D \quad (4)$$

Where a and b are determined by experimental data.

To combine linear and non-linear equations, all coefficients are multiplied by the drag coefficient as equation (5).

$$F_d U_{pore} = -\frac{1}{\rho}\nabla p = \frac{\mu}{\rho}\frac{1-n}{n}\left[A\frac{1-n}{n} + B\frac{\mathrm{Re}_p}{d_{pore}}\right]u_{pore} \quad (5)$$

Where F_d : drag coefficient (1/t), A: linear drag coefficient, B: non-linear drag coefficient, n: porosity coefficient, ρ fluid density, d_{pore} : diameter of aggregate, Re_p: Reynolds number in porous media, u_{pore} : fluid velocity in porous media.

Reynolds number in porous media is defined as equation (6).

$$\mathrm{Re}_p = \frac{\rho|u_{pore}|d_{pore}}{\mu} \approx \frac{\rho|U_D|d_{pore}}{n\mu} \quad (6)$$

Combining equations (4) and (5), the Forchheimer formula is derived as equation (7).

$$-\left(\frac{\partial p}{\partial x}\right) = A.|u_D|\mu\frac{(1-n)^2}{n^3} + B.|u_d|^2\rho\frac{(1-n)}{n^3} \quad (7)$$

Comparing equation (7) and equation (4), linear drag coefficient (A) and non-linear drag coefficient (B) are defined as equations (8) and (9), respectively.

$$A = a\frac{n^3}{\mu(1-n)^2} \quad (8)$$

$$B = b\frac{n^3}{\rho(1-n)} \quad (9)$$

In which, the coefficients A and B are dependent on grain material and calculated from experimental data and tables. Equations (8) and (9) are only applied when a full set of data of utilized grains is available. If the grain data is rare, the equations (10) and (11) are used to calculate the linear and non-linear drag coefficients.

$$A = \frac{180}{d_{pore}^{\ 2}} \quad (10)$$

$$B = \frac{\beta}{d_{pore}} \quad (11)$$

Where β is the fineness/hardness module varies from 1.8 to 4[15].

3. Numerical modeling

After presenting governing equations, according to the experimental modeling performed at Tarbiat Modares University, breakwater geometry, and prerequisite parameters of numerical modeling were inputted to the software.

3.1 Experimental model

In the experimental model, the pattern of Anzali port development project was used, and breakwater geometry was built (Figure 1).

Figure 1 Geometry of breakwater built in the lab [16]

The dimensions of breakwater were studied in the laboratory as shown in table 1[16].

Table 1 dimensions of different parts of studied breakwater

Breakwater height (cm)	30.5
Breakwater slope (°)	37
Filter thickness (cm)	3
Heel height(cm)	4
Heel slope (°)	34
Height of lower part of breakwater (cm)	21.2
The slope of the lower part of the breakwater (°)	8

Armour units used in the experimental model were Xbloc with the regular arrangement. Dimension sizes of armour units and their arrangement are shown in figure 2.

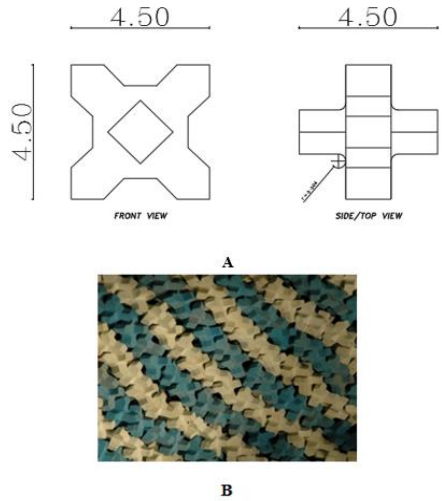

Figure 2 A) Xbloc size B) Xbloc arrangement [12]

To provide porous media, two types of grading with sizes of 4.5 cm and 1.2 cm were used for filter and core layers respectively to simulate actual condition.

Another experimental model requisite data for numerical modeling is the generated wave data. The irregular wave spectrum for wave characteristics presented in table 2, has been generated based on the Goda formula, in the laboratory. Using MATLAB code, the motions of the wave generator piston are defined in a way that generates desired wave spectrum [12] [17].

Table 2 irregular wave characteristics

Wave height (cm)	Wave period (s)
7.3	1.32
9.7	1.48
12.7	1.58

3.2 Breakwater modeling

Considering the geometry characteristics of the physical model; the geometry and layout used in AutoCAD software are shown in Figure 3.

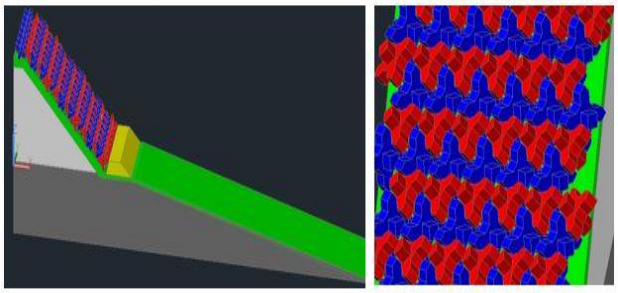

Figure 3 A) Breakwater geometry in numerical modeling B) Armour arrangement in numerical modeling

After designing the breakwater geometry in AutoCAD, the geometry was saved in STL format and inputted to FLOW-3D software.

Then, according to experimental data, the filter and core were modeled as porous media. Considering the grains' sizes, linear and non-linear Forchheimr drag coefficients of filter and core are calculated as equations 10 and 11:

Drag coefficient of filter:

$$\begin{cases} A = \dfrac{180}{d_{filter}^2} = \dfrac{180}{(4.5\times10^{-2})^2} = 8.88\times10^4 \\ B = \dfrac{\beta}{d_{filter}} = \dfrac{3}{4.5\times10^{-2}} = 66 \end{cases}$$

Drag coefficient of core:

$$\begin{cases} A = \dfrac{180}{d_{core}^2} = \dfrac{180}{(1.2\times10^{-2})^2} = 1.25\times10^6 \\ B = \dfrac{\beta}{d_{core}} = \dfrac{2}{1.2\times10^{-2}} = 166 \end{cases}$$

To model porous media in FLOW-3D software, it is necessary to introduce the porosity to media and then choose an appropriate way to model the porous media model. Then, the linear and non-linear drag coefficients are determined as in the calculations above.

After inputting the breakwater geometry to the software, the computational domain and boundary condition were determined. The dimensions of the computational domain were considered by 10 m length, 35 cm width, and 65 cm height as an experimental flume. To optimize the number of computational cells efficiently, four mesh blocks have been used for this domain. The dimensions of the blocks are shown in figure 4.

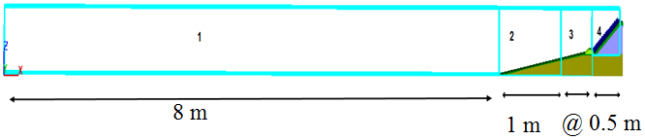

Figure 4 Segments of the computational domain

The boundary conditions are the basic parameters in the numerical simulation that should be noticed. After determining the computational domain, the boundary condition should be determined for each face of these four mesh blocks. The wave boundary condition, the wall boundary condition, the outflow boundary condition, and the symmetry boundary condition were used at the beginning of the first block, at the bottom of the blocks, at the end of the fourth block, and at other boundaries, respectively.

Since the purpose of this simulation is to generate an irregular wave similar to physical models; the only boundary condition that is necessary to be explained is the wave boundary condition used at the beginning of the first block.

The wave boundary condition needs a wave spectrum as an input to generate the irregular wave. Using Goda's equation, the wave spectrum is generated, considering the height and period of the experimental wave (Table 2).

Using Goda's equations, wave energy, S(f), was calculated for different values of wave frequency, f. To define irregular wave values of $2\pi f$ and S(f) were saved in a file with CSV format and then were inputted into the software [12].

3.3 Meshing and sensitivity analysis of modeling

Determining the best mesh is one of the most important steps in numerical studies because the coarse mesh could result in larger gradients of changes. It is not possible to reach the correct answer. So, mesh refinement is needed to correctly capture the changes in regions which are subjected to harsh gradients and to reach a more accurate answer in a computational cell. But it should be noted that this mesh refinement should be performed carefully, since it may increase the number of computational cells as well as the calculation time.

After physical modeling, it is necessary to make the mesh efficient. To assess the sensitivity of the numerical model than the number of computational cells, a large number of modeling was performed, and finally, the cell sizes of different blocks were obtained as shown in Table 3[12].

Table 3 mesh characteristics

Mesh block	1	2	3	4
Mesh size (mm)	22.5	12.9	8.6	7.04

As it is seen in table 3, the size of the computational cell in the range of the breakwater geometry cell was considered smaller to perform modeling more sensitive. Also, the size of the computational cell was considered 1.2-1.8 times larger than the adjacent block. The shape of breakwater after rendering in FLOW-3D demonstrated in figure 5.

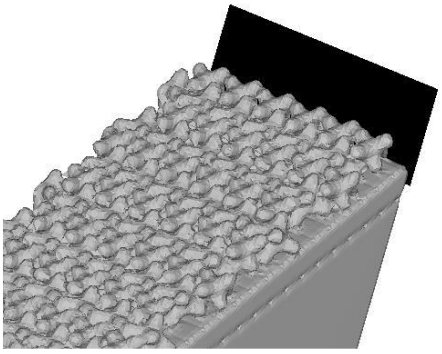

Figure 5 breakwater after rendering in FLOW-3D

3.4 Calibration and validation using experimental data

After defining the breakwater and details of modeling in the software, modeling was performed. To be assured of the results' accuracy, wave overtopping resulted from three waves listed in table 2 was compared with experimental results. There were no specific details about the porosity of filter layers and core in the experimental model. To calibrate the numerical model, the simulation was performed for different porosities. Comparing the overtopping results from numerical modeling with mean overtopping discharge values of the experimental study, clearly shows that the numerical modeling results with a porosity value of 0.45 have higher precision than experimental data. Therefore, the porosity value of 0.45 was used for validation[12].

Validation settings were as follows, water height at the structure: 40 cm, turbulence model: RNG, porosity value: 0.45, simulation time: 100 sec. A comparison between mean overtopping discharge results of numerical modeling and mean overtopping discharge of experimental studies for different wave heights is outlined in table 4.

Table 4. Validation results for different wave characteristics

Wave height (cm)	7.3	9.7	12.7
Experimental wave overtopping (liter/s)	1.09×10^{-4}	2.406×10^{-3}	6.125×10^{-3}
Numerical wave overtopping (liter/s)	9.56×10^{-5}	2.07×10^{-3}	6.97×10^{-3}
Normal error (%)	-14	-16	12

Table 4 shows that mean overtopping discharge results have higher precision than experimental results. Also, the numerical modeling error was 12-16 %. This was acceptable considering the differences between numerical and experimental modeling characteristics and also numerical modeling errors. To assess the simulation time effect on results, duration was increased to 150 s and decreased to 50 s, and the mean overtopping discharge values of 150 s and 50 s were compared. The results for the wave height of 12.7 cm are shown in table 5.

Table 5 time effect on wave overtopping

Time (second)	50	100	150
mean overtopping discharge (liter/s)	7.123×10^{-3}	6.97×10^{-3}	6.88×10^{-3}

This comparison represents that mean overtopping discharge is decreased slightly with increasing duration. This is because of wave-wave interaction. In the first 50 s, since new waves are shaping up and decrease in wave height cause of wave-wave interaction is less, the results of mean overtopping discharge for 100 and 150 s have been more.

One of the important outputs of software is overtopping schema at the structure. The moment of maximum overtopping for different wave heights was as shown in figure 6.

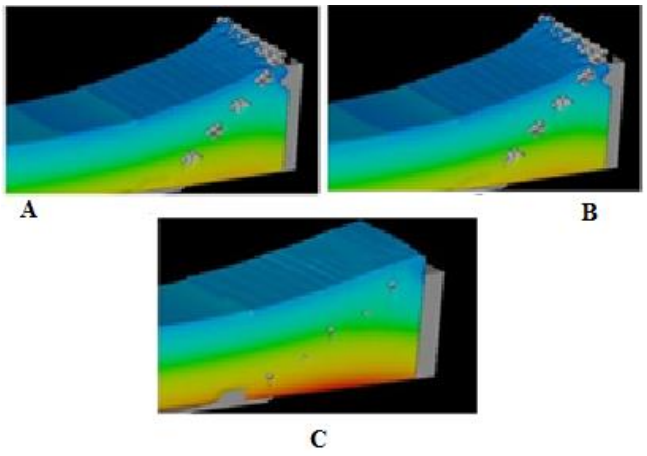

Figure 6 over topping moment for different wave heights Hs=7.3 cm B) Hs=9.7 cm C) Hs=12.7 cm

4. Modeling armour type and arrangement effects

To assess armour type and arrangement effects on overtopping, for three breakwaters with different armour blocks: Xbloc, Antifer, tetrapod- and different arrangements, modeling was performed. Results of overtopping were compared to characterize the best performance of different armour types and arrangements to decrease the overtopping.

4.1 X-block armour

X-block armour was modeled as one-layer and two types of arrangements, regular and irregular. For numerical modeling, it was necessary to build the breakwater geometry and arrangements in AutoCAD. In the present study, regular and irregular arrangements were based on experimental data from Piter et al. study, as shown in figure 7.

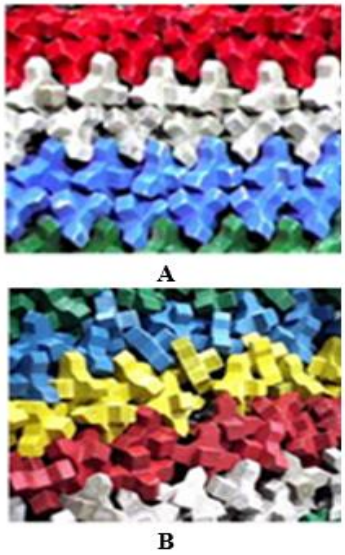

Figure 7 Xbloc arrangements in laboratory A) regular arrangement B) irregular arrangement [18]

Figure 8 shows the modeled regular and irregular arrangements of Xbloc in AutoCAD.

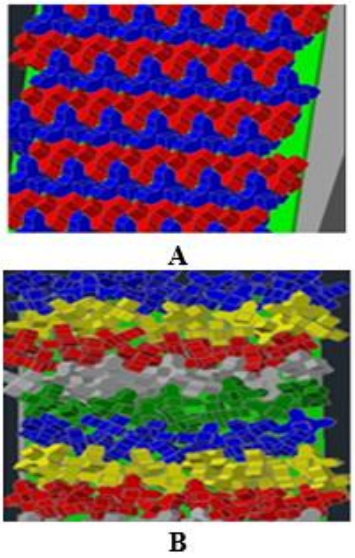

Figure 8 Xbloc arrangements in numerical modeling A) regular arrangement B) irregular arrangement

After building the model geometry and defining the numerical parameters as previous, modeling was performed for rubble mound breakwater segments with slope range of 1-1.5, porosity value of 0.25, freeboard value of 7 cm, wave heights characteristics of table 2 and the A and B types of arrangement as shown in figure 8. The results are represented in figure 9.

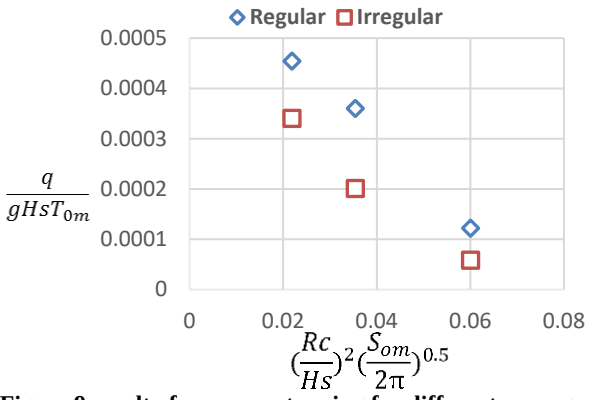

Figure 9 result of wave overtopping for different arrangement of Xbloc

The modeling results showed that the overtopping increased with increasing wave height as previously. Using the irregular arrangement of armour blocks, overtopping was decreased. That is because of more wave energy damp between irregularly arranged blocks. At the wave height of 7.3 cm, overtopping discharge at the breakwater with the irregular arrangement is half of the corresponding value at the breakwater with regular arrangement. At the wave height of 9.7 cm, this was more than half, while at 12.7 cm the overtopping was approximately equal for regular and irregular arrangements. The changes trend shows that irregular arrangement has a high impact on overtopping decrease at small wave heights. When the wave height is increased, the impact of irregular arrangement is decreased.

4.2 Antifer armour

This armour is modeled as two-layers. For numerical modeling, it was necessary to build the breakwater geometry and arrangements in AutoCAD.

In the laboratory, the physical modeling performed for different arrangements of Antifer armour, However, for numerical modeling, two arrangements used as shown in figure 10, which were studied at Delft University of Technology[19].

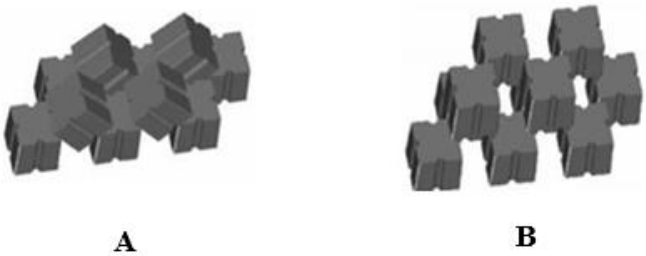

Figure 10 Antifer arrangements in laboratory A) type A B) type B[19]

Based on an experimental schema, as shown in figure 10, the A and B types of Antifer armour arrangements were built-in AutoCAD, as shown in figure 11.

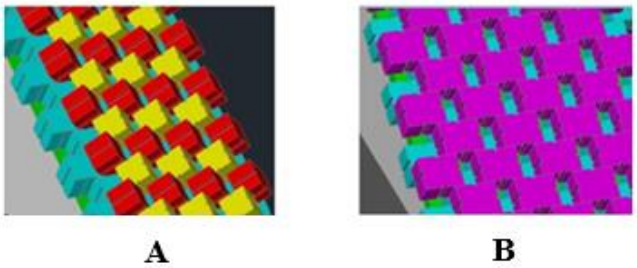

Figure 61 Antifer arrangements in numerical modeling A) type A B) type B

After preparing the model geometry and defining the numerical parameters as previous, modeling was performed for rubble mound breakwater segments with slope range of 1-1.5, porosity value of 0.25, freeboard value of 7 cm, wave heights characteristics of table 2 and the A and B types of arrangement as shown in figure 11. The results are represented in figure 12.

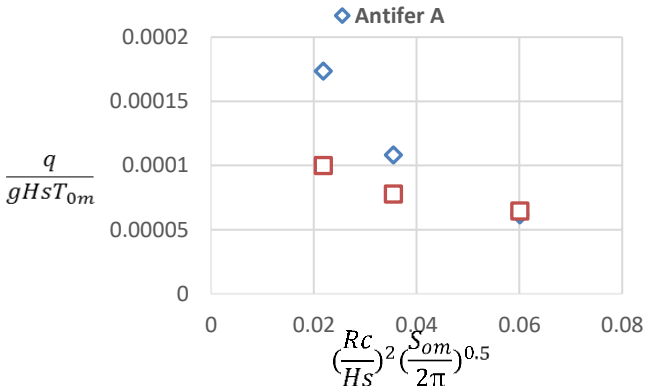

Figure 72 wave overtopping results for different arrangements of Antifer

The results represent that by using a B-type arrangement, the overtopping is decreased. This is because of the more porosity of B-type than A-type. Because of more distance and porosity in B-type than A-type, this arrangement has more porosity.

4.3 Tetrapod armour

Similar to previous armours, in this section, the breakwater geometry and arrangements should be modeled in AutoCAD. The arrangements of tetrapod were based on Fabio's experimental data that was fulfilled in the University of Lisbon, as shown in figure 13[20].

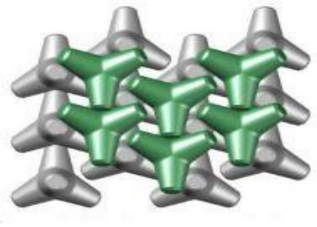

Figure 83 Tetrapad arrangement in a laboratory [20]

Based on the experimental schema, as shown in figure 13, tetrapod armour arrangements were modeled in AutoCAD, as shown in figure 14.

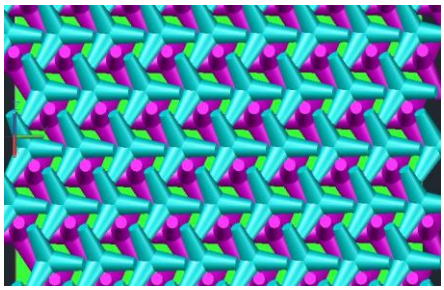

Figure 94 Tetrapad arrangement in numerical modeling

After modeling geometry and characterizing the numerical parameters as previous, modeling was performed for rubble mound breakwater segments with a slope range of 1-1.5, porosity value of 0.25, freeboard value of 7 cm, wave heights characteristics of table 2, and with an arrangement as shown in figure 14. The results are represented in figure 15.

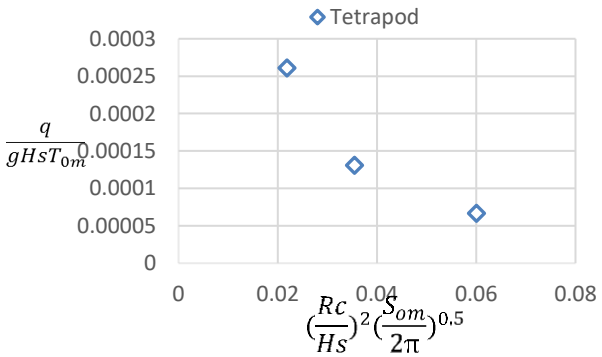

Figure 105 result of wave overtopping for Tetrapod

4.4 Comparison of different Armour arrangements

To better represent, figures 9, 12, and 15 have been aggregated in figure 16.

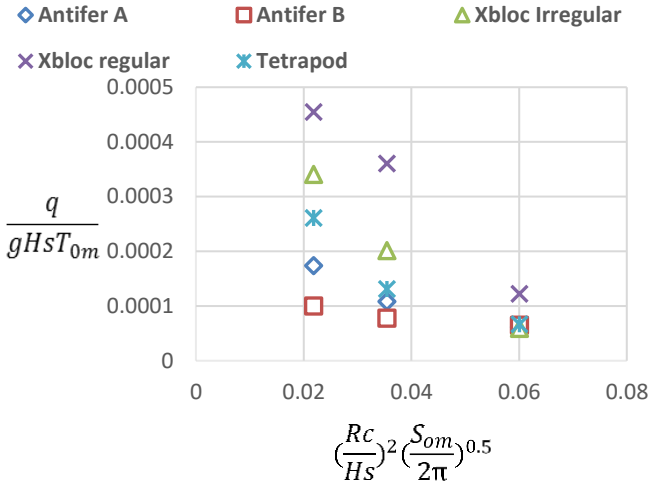

Figure 116 wave overtopping results for different armour types and arrangements

As it is obvious in figure 16, the B-type arrangement of Antifer has the lowest overtopping and the most overtopping belongs to the regular arrangement of Xbloc. Tetrapod blocks have more overtopping than two arrangements of Antifer and lower overtopping than two arrangements of X-block. Also, changing Armour blocks effect at high wave heights is observed while there is no significant difference at small wave heights. The only difference is related to the overtopping discharge of regular and irregular arrangements of X-block.

5. Conclusion

In the present study, first of all, the irregular wave spectrum on porous media of breakwater and armour blocks using FLOW-3D software was simulated. After comparing the numerical and experimental modeling results and ensure about numerical modeling accuracy for prefabricated concrete X blocks, Antifer and tetrapod, and different arrangements of these blocks, the modeling was performed. Type and arrangement effects of the blocks were compared. Irregular arrangements have a high impact on overtopping decrease at small wave heights. When the wave height is increased, the impact of irregular arrangement is decreased. Using the B-type arrangement of Antifer armour blocks, the overtopping discharge will be decreased because of more porosity of B arrangement than A. A small wave heights, using A-type or B-type arrangements of Antifer makes no significant change on overtopping but in high wave heights, the B-type arrangement has lower overtopping. Tetrapod armour has more overtopping than Xbloc and is lower than Antifer.

Between different segments and arrangements that used, the lowest overtopping occurred for B arrangement of Antifer armours and the most overtopping occurred for the regular arrangement of X-blocks.

6. References

1- A.Farhadzadeh, M.shafee far, "*Analytical study of existing models for measuring wave overtopping in coastal structures*". Eighth Conference on Marine Industries. Iran, Bushehr.

2- K. Hu, C. G. Mingham, and D. M. Causon, "*Numerical simulation of wave overtopping of coastal structures using the non-linear shallow water equations*," Coast. Eng., vol. 41, no. 4, pp. 433–465, 2000.

3- P. Besley, T. Stewart, and N. W. H. Allsop, "*Overtopping of vertical structures: new prediction methods to account for shallow water conditions*," Proc. Coastlines, Struct. Break. London, UK, pp. 46–57, 1998.

4- Y. Goda, "*Random seas and design of maritime structures*". *World Scientific, 2010.*

5- *T. S. Hedges, M. T. Reis, and M. W. OWEN, "Random Wave Overtopping Of Simple Sea Walls: A New Regression Model.*," Proc. ICE-Water Marit. Energy, vol. 130, no. 1, pp. 1–10, 1998.

6- J. W. van der Meer, J. P. F. M. Janssen, and D. Hydraulics, "*Wave run-up and wave overtopping at dikes and revetments*". Delft Hydraulics, 1994.

7- N. Kobayashi and A. Wurjanto, "*Wave overtopping on coastal structures*," J. Waterw. Port, Coastal, Ocean Eng., vol. 115, no. 2, pp. 235–251, 1989.

8- Marayama and Hiraishi, "*presented a numerical model for calculation of over topping discharge for a vertical breakwater in multi direction wave",*The basic assumption is that the overtopping discharge can be described by a weir expression as suggested by Kikkawa et al 1988." 1988.

9- M. D. Torrey, L. D. Cloutman, R. C. Mjolsness, and C. W. Hirt, "*NASA-VOF2D: a computer program for incompressible flows with free surface*s," NASA STI/Recon Tech. Rep. N, vol. 86, p. 30116, 1985.

10- J. M. Sicilian, C. W. Hirt, and R. P. Harper, "*FLOW-3D: Computational modeling power for scientists and engineers,"* Flow Sci. report, FSI-87-QO-l, 1987.

11- F. Dentale, G. Donnarumma, and E. E. P. Carratelli, "*Rubble Mound Breakwater: Run-Up, Reflection and Overtopping by Numerical 3D Simulation*," flow3d.com, 2012.

12- Ghasemi A, Shafiee far M, Panahi R. *"Numerical Simulation of Wave Overtopping From Armour Breakwater by Considering Porous Effect"*. marine-engineering. 2016; 11 (22) :51-60.

13- Marashian S M, Adjami M, Rezaee Mazyak A. *"Numerical Simulation of Wave Overtopping Over Composite Berm Breakwater"* . marine-engineering. 2019; 15 (29) :25-38

14- Amirabadi R, Rezaee mazyak A, Ghasemi A. *"Numerical Modeling Investigation of Irregular Wave Interaction with Perforated Caisson Breakwater"*. marine-engineering. 2018; 14 (27) :69-79

15- F. Science, "*FLOW-3D Documentation*," 2012.

16- Mousavi B, Saadatkhah N,A Haj Momeni. *"Stability Evaluation of Breakwater Inner Slope under Overpassing, Based on Physical Modeling and Comparing with Experimental Relations (Case Study: Breakwaters in Anzali Port Development Plan)"*. 2011; 10th international conferancces of coastal, ports and, marine sutrucutres, Iran, Tehran,.

17- Y. Goda, "*Statistical variability of sea state parameters as a function of wave spectrum*," Coast. Eng. Japan, vol. 31, no. 1, pp. 39–52, 1988.

18- P. Bakker, M. Klabbers, M. Muttray, and A. van den Berge, "*Hydraulic performance of Xbloc® armour units, in 1st international conference on coastal zone management and engineering in the Middle East"*, 2005.

19- A. B. Frens, "*The impact of placement method on Antifer-block stability*", Delft Univ. Technol. Delft, 2007.

20- J. Fabião, A. T. Teixeira, and M. Araújo, "*hydraulic stability of tetrapod armour layers-physical model study*", Instituto Superior Técnico, Universidade Técnica de Lisboa 2009.